Brassica juncea 3-hydroxy-3-methylglutaryl (HMG)-CoA synthase 1: expression and characterization of recombinant wild-type and mutant enzymes

Dinesh A. NAGEGOWDA*, Thomas J. BACH† and Mee-Len CHYE*[1]

*Department of Botany, The University of Hong Kong, Pokfulam, Hong Kong, China, and †Centre National de la Recherche Scientifique, UPR 2357, Institut de Biologie. Moléculaire des Plantes, 28 rue Goethe, 67083 Strasbourg Cedex, France

3-Hydroxy-3-methylglutaryl (HMG)-CoA synthase (HMGS; EC 2.3.3.10) is the second enzyme in the cytoplasmic mevalonate pathway of isoprenoid biosynthesis, and catalyses the condensation of acetyl-CoA with acetoacetyl-CoA (AcAc-CoA) to yield *S*-HMG-CoA. In this study, we have first characterized in detail a plant HMGS, *Brassica juncea* HMGS1 (BjHMGS1), as a His_6-tagged protein from *Escherichia coli*. Native gel electrophoresis analysis showed that the enzyme behaves as a homodimer with a calculated mass of 105.8 kDa. It is activated by 5 mM dithioerythreitol and is inhibited by F-244 which is specific for HMGS enzymes. It has a pH optimum of 8.5 and a temperature optimum of 35 °C, with an energy of activation of 62.5 $J \cdot mol^{-1}$. Unlike cytosolic HMGS from chicken and cockroach, cations like Mg^{2+}, Mn^{2+}, Zn^{2+} and Co^{2+} did not stimulate His_6–BjHMGS1 activity *in vitro*; instead all except Mg^{2+} were inhibitory. His_6–BjHMGS1 has an apparent $K_{m\text{-}acetyl\text{-}CoA}$ of 43 μM and a V_{max} of 0.47 $\mu mol \cdot mg^{-1} \cdot min^{-1}$, and was inhibited by one of the substrates (AcAc-CoA) and by both products (HMG-CoA and HS-CoA). Site-directed mutagenesis of conserved amino acid residues in BjHMGS1 revealed that substitutions R157A, H188N and C212S resulted in a decreased V_{max}, indicating some involvement of these residues in catalytic capacity. Unlike His_6–BjHMGS1 and its soluble purified mutant derivatives, the H188N mutant did not display substrate inhibition by AcAc-CoA. Substitution S359A resulted in a 10-fold increased specific activity. Based on these kinetic analyses, we generated a novel double mutation H188N/S359A, which resulted in a 10-fold increased specific activity, but still lacking inhibition by AcAc-CoA, strongly suggesting that His-188 is involved in conferring substrate inhibition on His_6–BjHMGS1. Substitution of an aminoacyl residue resulting in loss of substrate inhibition has never been previously reported for any HMGS.

Key words: *Brassica juncea*, enzyme kinetics, HMG-CoA synthase, *in vitro* mutagenesis, isoprenoid biosynthesis, substrate inhibition.

INTRODUCTION

Plants synthesize a myriad of isoprenoids, which play an essential role in various cellular functions such as photosynthesis (carotenoids, chlorophylls, phylloquinones), respiration (ubiquinone), membrane architecture (sterols and triterpenoids), regulation of growth and development (gibberellic acids, abscisic acid, brassinosteroids, certain cytokinins, e.g. isopentenyl adenosine), and defence against pathogen attack (mono-, sesqui- and di-terpenoid phytoalexins), or serve as chemical signals [1,2]. All these entities are derived from the universal precursor isopentenyl diphosphate (IPP, also referred to as 'activated' isoprene) and its isomer dimethylallyl diphosphate (DMAPP). In higher plants two biosynthetic pathways are responsible for the synthesis of these precursors: the classical mevalonate pathway ([1,3] and literature cited therein) and the recently discovered methylerythritol phosphate (MEP) pathway [4,5]. The mevalonate pathway operates in the cytosol, whereas the non-mevalonate MEP or Rohmer pathway is confined to plastids [6,7].

During the course of evolution, higher plants have maintained both pathways, whereas, with the exception of some species of Actinomycetes studied so far, other organisms use either the MEP pathway, for example green algae and many bacteria, or the mevalonic acid (MVA) pathway, such as archaebacteria, certain eubacteria, fungi and animals [7]. In higher plant cells, the cytosolic MVA pathway provides the precursor molecules for sterols, ubiquinone, and certain sesquiterpenes, besides delivering the isoprenic units for farnesylation of a series of proteins, and as the starter unit for the formation of dolichols and polyprenols. MVA biosynthesis appears to be essential for cell-cycle progression and viability of plant cells [8,9], but to some extent the two compartmentalized pathways seem to conspire, and evidence for metabolic cross-talk has been presented [10,11].

MVA biosynthesis is a complex process involving a series of three enzyme-catalysed reactions. Three molecules of acetyl-CoA are converted into one molecule of *S*-3-hydroxy-3-methylglutaryl-CoA (HMG-CoA) by the sequential action of two enzymes: acetoacetyl (AcAc)-CoA thiolase (AACT; EC 2.3.1.9) catalysing a thermodynamically unfavourable Claisen-type condensation of two acetyl-CoA molecules to form the intermediate AcAc-CoA [12,13], and 3-hydroxy-3-methylglutaryl-CoA synthase (HMGS, EC 2.3.3.10, formerly EC 4.1.3.5), catalysing a thermodynamically favourable aldol condensation of one molecule of AcAc-CoA with acetyl-CoA to form one molecule of *S*-HMG-CoA [12,14–16]. The combination of these two reactions favours the overall reaction from acetyl-CoA to HMG-CoA, which is

Abbreviations used: AcAc-CoA, acetoacetyl-CoA; AACT, AcAc-CoA thiolase; BjHMGS1, *Brassica juncea* HMGS1; DMAPP, dimethylallyl diphosphate; DTE, dithioerythritol; DTT, dithiothreitol; DX, 1-deoxy-D-xylulose; HMG-CoA, 3-hydroxy-3-methylglutaryl-CoA; HMGR, 3-hydroxy-3-methylglutaryl-CoA reductase; HMGS, HMG-CoA synthase; HS-CoA, reduced CoA; K_i, inhibition constant; IPP, isopentenyl diphosphate; IPTG, isopropyl β-D-thiogalactoside; MEP, methylerythritol phosphate; MVA, mevalonic acid; NADPH, β-nicotinamide adenine dinucleotide phosphate reduced; Ni^{2+}-NTA, Ni^{2+}-nitrilotriacetic acid; S359A etc., Ser → Ala substitution etc.

[1] To whom correspondence should be addressed (email mlchye@hkucc.hku.hk).

the substrate of NADPH-dependent, membrane-bound HMG-CoA reductase (HMGR, EC 1.1.1.34), the enzyme that generates MVA and being generally considered to catalyse the key regu–latory step, for instance in phytosterol biosynthesis [1,17].

The formation of HMG-CoA from acetyl-CoA and AcAc-CoA by the 'condensing enzyme' HMGS has been well studied, initially in yeast [18,19]. These initial studies with the partially purified yeast enzyme revealed that the free carboxyl end of HMG-CoA did arise from hydrolysis of the thioester bond of acetyl-CoA [18,19]. In follow-up studies, again using purified yeast HMGS, Stewart and Rudney [20,21] proved that the CoA moiety of HMG-CoA stemmed from AcAc-CoA, the CoA part of the molecule being radiolabelled; this label was found in the product HMG-CoA. Incubation of the enzyme with [1-^{14}C]acetyl-CoA led to a covalently bound acetyl–enzyme intermediate; however, under those conditions there was no significant HMG acid or HMG-CoA found to be bound, indicative of a rather rapid release of the reaction product from the enzyme. These initial studies were hampered by the presence of contaminating AACT, a problem that could be resolved by establishing a new purification protocol for bakers' yeast HMGS [22], which led to an enzyme preparation essentially free of AACT, used in a series of very extensive kinetic analyses [22–24]. Miziorko and Lane [25] provided clear evidence for the acetylation of HMGS by acetyl-CoA to constitute the rate-limiting step for the overall reaction to HMG-CoA, confirming the observations with yeast enzyme [23,24], suggesting a rapid hydrolysis of the HMG-CoA-*S*-enzyme intermediate.

The purification of a plant HMGS has not been achieved, although HMGS activity has been demonstrated in crude or partially-purified extracts from several plant species [26–28]. Some evidence for a single protein involved in the conversion of acetyl-CoA into HMG-CoA has been reported in radish seedlings [29] but it seems likely that a plant-specific enzyme interferes with the usual radioactive test system based on that of Clinkenbeard et al. [16], thereby masking true HMGS activity. In *Catharanthus roseus*, the enzymes AACT and HMGS exhibited similar chromatographic behaviour [27], thus making their complete isolation from each other practically impossible, similar to the problems initially encountered with the yeast enzyme [20,21]. In a more recent study it was reported that HMGS activity is positively correlated with rubber content in *Hevea brasiliensis*, suggesting a regulatory role of this enzyme in the diurnal variation of rubber biosynthesis [28] in parallel with HMGR activity. A fortuitously isolated cDNA encoding HMGS from *Arabidopsis* was reported to functionally complement yeast mutants (*erg11* and *erg13*) defective for HMGS [30]. *HMGS* mRNA from *Pinus sylvestris* is induced by ozone [31]. An *HMGS* gene has also been cloned from *H. brasiliensis* [32].

Current knowledge on HMGS kinetics is derived from yeast, human, rat, avian, and insect HMGS; such reports are lacking on plant HMGS. Previously we have isolated four isogenes encoding HMGS from *Brassica juncea* and showed that *HMGS* gene expression is developmentally regulated in flower, seed and seedling, with highest values reached during early development [33]. In the present study, we report the expression, purification and enzymic characterization of *B. juncea* HMG-CoA synthase, the second enzyme in the cytoplasmic mevalonate pathway of isoprenoid biosynthesis, and the first characterized plant HMGS. In addition, site-directed mutational analysis of thirteen evolutionarily conserved amino acid residues (Tyr-35, Arg-77, Lys-88, Ser-89, Lys-90, Asn-115, Cys-117, Tyr-118, Arg-157, His-188, Cys-212, Ser-356 and Ser-359) was conducted to investigate their possible involvement in the enzyme's catalysis. All mutants, except those corresponding to Cys-117, Tyr-118 and Cys-212, have never been previously investigated in any HMGS.

EXPERIMENTAL

Materials

Restriction endonucleases and DNA-modifying enzymes were purchased from Boehringer Mannheim, Sequenase™ Version 2.0 DNA Sequencing Kit from Amersham Biosciences, and the QuikChange™ site-directed mutagenesis kit from Stratagene. Oligonucleotides for site-directed mutagenesis were custom-synthesized by Life Technologies Inc. Isopropyl β-D-thiogalactoside (IPTG), AcAc-CoA, HMG-CoA, [^{14}C]acetyl-CoA, dithioerythritol (DTE) and BSA were purchased from Sigma, SDS/PAGE molecular-mass standards from Bio-Rad, Ni^{2+}-nitrilotriacetic acid (Ni^{2+}-NTA) resin from Qiagen and *Escherichia coli* BL21 Star (DE3) pLysS from Invitrogen.

Bacterial strains and plasmids

E. coli DH5α was used for propagation of plasmids. *E. coli* BL21 Star (DE3) pLysS (Invitrogen) was used to express the His_6-tagged wild-type and mutant enzymes. The plasmid pET3a (Novagen), was used as the expression vector for overexpression of wild-type and mutant enzymes from the T7 promoter for kinetic analysis.

Construction of the His_6–BjHMGS1 (*B. juncea* HMGS1) expression vector

The open reading frame of *BjHMGS1* was derived by PCR-amplification using plasmid pBj49, which contains the full-length 1.68 kb BjHMGS1 cDNA [33] using forward primer 5′-GGA-TCC**CATCATCATCATCATCAT***ATG*GCGAAGAACGTAGG-GATAT-3′ (*Bam*HI site underlined, His_6-tag-encoding DNA in bold and BjHMGS1 start codon in italics) and reverse primer 5′-GGATCC**TCA**GTGTCCATTGGTTATGGAGCC-3′ (*Bam*HI site underlined and stop codon in bold). The amplified DNA was cloned into the prokaryotic expression vector pET-3a (Novagen), yielding plasmid pBj75. This cloning process introduced a *Bam*HI site and a His_6-tag 5′ to the BjHMGS1 cDNA and a *Bam*HI site immediately downstream from the translation stop codon. The entire length of PCR-amplified DNA was confirmed by nucleotide sequence analysis.

Expression and purification of recombinant His_6–BjHMGS1

Single colonies of cells harbouring recombinant DNA were picked from plates containing Luria–Bertani medium with ampicillin (50 μg/ml) and chloramphenicol (35 μg/ml) for inoculation of 5 ml cultures. These cultures were grown overnight at 37 °C before use in inoculating 100 ml cultures in Luria–Bertani medium containing the appropriate antibiotics. Cultures were grown at 37 °C until $D_{600} = 0.4$, as measured using a UV-spectrophotometer (Shimadzu Model UV-1206). IPTG was then added to a final concentration of 0.5 mM, and the culture further grown for 4 h. The cells were harvested by centrifugation at 5000 ***g*** at 4 °C for 10 min and stored at − 20 °C. For protein extraction, cell pellets were thawed on ice and resuspended in 4 ml of native lysis buffer (50 mM NaH_2PO_4, 300 mM NaCl, 10 mM imidazole, pH 8.0) and then powdered in liquid nitrogen. The homogenate was centrifuged at 27 000 ***g*** for 30 min and passed through a column (0.8 × 4 cm, Bio-Rad, Cat. No. 731-1550) packed with 1 ml of Ni^{2+}-NTA agarose, equilibrated with lysis buffer. Proteins bound to the Ni^{2+}-NTA agarose column were washed once with 4 ml of native washing buffer 1 (50 mM NaH_2PO_4, 300 mM NaCl, 0.8 mM imidazole, pH 8.0), twice with 4 ml of native washing buffer 2 (50 mM NaH_2PO_4, 300 mM NaCl, 8 mM imidazole, pH 8.0) and twice with 4 ml of native washing buffer 3 (50 mM NaH_2PO_4, 300 mM NaCl, 50 mM imidazole, pH 8.0). Finally the

Table 1 Synthetic oligonucleotide primers used for *in vitro* site-directed mutagenesis

Codons for the changed amino acids are underlined. Nucleotides represented in italics indicate the product point mutations.

Primer name	Primer sequence
Y35A	5′-GCAAAGGGAAA*GCC*ACCATTGGAC-3′
R77A	5′-CAAGCAAATTGGG*GCT*CTTGAAGTAGGC-3′
K88A	5′-GACTGTCATTGAC*GCG*AGCAAGTCCATC-3′
S89A	5′- CTGTCATTGACAAG*GCC*AAGTCCATCAAAAC -3′
K90A	5′- CATTGACAAGAGC*GCG*TCCATCAAAACC -3′
N115A	5′- CCAATGCTTGT*GCT*GGTGGAACTGC -3′
C117A	5′-CGACCAATGCT*GCT*TATGGTGGAACTG-3′
Y118A	5′-CCAATGCTTGT*GCT*GGTGGAACTGC-3′
R157A	5′- GAAGGGCCCGCA*GCG*CCCACTGGAGG -3′
H188N	5′- GAAGCCACATGGCT*AAT*GTCTATGACTTTTAC -3′
C212S	5′- CTTTCACAGACAT*CCT*ACCTTATGGC -3′
S356A	5′- GTGGTTATGTTC*GCA*TATGGAAGTGG -3′
S359A	5′- GTTCTCATATGGA*GCT*GGTTCAACCGC -3′

His_6–BjHMGS1 was eluted using 4×0.5 ml of native elution buffer (50 mM NaH_2PO_4, 300 mM NaCl, 80 mM imidazole, pH 8.0). The fractions containing His_6–BjHMGS1 were pooled and dialysed overnight against 50 mM Tris buffer, pH 7.5.

Construction of BjHMGS1 mutants by *in vitro* site-directed mutagenesis

Plasmid pBj75 was used as a mutagenesis template for generating mutant derivatives of recombinant His_6–BjHMGS1. Plasmid pBj89 having a S359A (Ser → Ala) substitution was used as template to create the H188A/S359A double mutant in pBj110. The QuikChange site-directed mutagenesis kit (Stratagene) was used to obtain mutant derivatives, which were subsequently verified by nucleotide sequence analysis using the Sequenase™ Version 2.0 DNA Sequencing Kit (Amersham Biosciences). The primer pairs used in site-directed mutagenesis are listed in Table 1. Mutagenesis was carried out by PCR using *Pfu* DNA polymerase according to the manufacturer. The amplification procedure included 16 cycles of denaturation (95 °C for 30 s), annealing (55 °C for 1 min) and extension (68 °C for 12 min). The amplified product was treated with *Dpn*I to remove template DNA and the mutated DNA was used in transformation of DH5α competent cells. The mutations were confirmed by nucleotide sequence analysis. *E. coli* BL21 Star (DE3) pLysS was transformed with the verified plasmids for subsequent expression of mutant His_6–BjHMGS1 enzymes.

Protein analysis

Protein concentrations were determined by the method of Bradford [34]. Equal amounts of protein (10 μg) were analysed using SDS/PAGE (10 % gel) at pH 8.3; the gel was stained with Commassie Blue or used for Western-blot analysis [35] by cross-reaction with anti-peptide antibodies raised in rabbit (Mimotopes, Clayton, Vic., Australia) against a synthetic peptide (SLYRRFY-GKKGDD) corresponding to amino acids 442–454 (single letter coding) of BjHMGS1 [33]. The molecular mass of the purified His_6–BjHMGS1 was determined by non-denaturing PAGE (6–12 % gels) according to the method of Gallangher [36].

HMGS assay

The enzyme assay was based on a method developed for avian HMGS [15], which was modified as follows: 15 μl of enzyme solution was added to 35 μl of a mix containing 25.6 μl of 50 mM Tris buffer (pH 7.5), 2.5 μl of 0.1 M DTE, 2.5 μl of BSA stock solution (50 mg/ml), 2.0 μl solution at 10 μCi/ml of [^{14}C]acetyl-CoA (Sigma) in 50 mM KH_2PO_4, pH 4.5 (44000 d.p.m., final concentration of 9 μM in the assay), and 2.4 μl of unlabelled AcAc-CoA (Sigma) in 50 mM KH_2PO_4 (pH 4.5) to give an equimolar concentration in the assay. After a 10 min incubation at 30 °C (linear range), the reaction was stopped by addition of 6 M HCl. Incubation was continued for 30 min and then solutions were transferred to scintillation vials, in which the samples were heated at 110 °C for at least 3 h. Under these conditions thioesters are hydrolysed, [^{14}C]acetate from unreacted [^{14}C]acetyl-CoA is volatile and only [^{14}C]HMG acid, from enzymically formed HMG-CoA, would remain in the vials. Hence, incorporation of radioactivity into heat- and acid-stable product indicates HMGS activity. To re-dissolve the [^{14}C]HMG acid, 0.4 ml of water was added followed by incubation at 22 °C for 10 min. After addition of 5 ml of scintillation cocktail (ReadyGel, Beckman), the samples were vigorously vortex-mixed. After 30 min, radioactivity was determined using a liquid-scintillation counter, type Minaxi Tri-Carb 4000 (Packard), with automatic quench correction by the external standard method. Appropriate controls were run in the absence of enzyme protein and in the presence of boiled protein. A linear activity range was determined for each protein, testing 20 ng to 1 μg protein per assay. For mutant K90A that showed no activity within this range, assays were carried out using up to 5 μg of protein per assay in the reaction.

Kinetic analysis on purified wild-type His_6–BjHMGS1

Purified His_6–BjHMGS1 and its mutants were used for all kinetic parameter determinations employing the standard radiometric assay [15]. Standard kinetic parameters were estimated using non-linear regression analysis of rate data. For evaluation of the pH dependence of wild-type His_6–BjHMGS1, the radioactive assay was modified to contain 50 mM Tris/HCl (pH ranging from 6–11), whereas for temperature dependence, the assay was conducted between 10 and 50 °C with 5 °C increments in the presence of equimolar concentrations of [^{14}C]acetyl-CoA and AcAc-CoA. To evaluate the requirement of divalent cations, the assay was carried out in the presence of 0.5–10 mM concentrations of Mg^{2+}, Mn^{2+}, Co^{2+} and Zn^{2+}. For investigating the effect of F-244 on His_6–BjHMGS1 activity, assays were carried out in the presence of 0–100 nM F-244. For all the assay systems, a linear activity range of His_6–BjHMGS1 was used, and an average of 2–3 separate assays was taken.

For determinations of the kinetic parameters V_{max} and K_m, assays were performed under the standard conditions, as described above, with concentrations of both substrates varying between 2 and 80 μM. The kinetic data were fitted to the Michaelis–Menten equation, and the kinetic parameter values for both substrates were determined from secondary plots of the slopes and intercepts versus the reciprocal of the fixed substrate concentration.

Acetyl-CoA hydrolase activity

Acetyl-CoA hydrolase activity of wild-type and mutant synthases was measured by monitoring enzyme-dependent depletion of [^{14}C]acetyl-CoA after conversion of residual substrate into acid-stable [^{14}C]citrate, using excess citrate synthase and oxaloacetate [37].

CD spectroscopy

CD spectroscopy for wild-type His_6–BjHMGS1 and its mutant forms was carried out at 22 °C using a spectropolarimeter

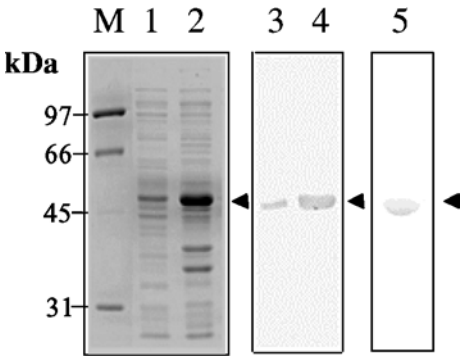

Figure 1 Expression of His_6–BjHMGS1 in *E. coli* BL21 Star (DE3) pLysS cells

Coomassie Blue-stained gel of soluble protein from *E. coli* bearing pBj75 before induction with 0.5 mM IPTG (lane 1) and 4 h post-induction (lane 2). Western-blot analysis using anti-peptide antibodies against His_6–BjHMGS1 using similar cultures before (lane 3) and after (lane 4) IPTG-induction. SDS/PAGE of Ni^{2+}-NTA purified His_6–BjHMGS1 stained with Commassie Blue (lane 5). The arrowheads denote the 53 kDa His_6–BjHMGS1. M, molecular-mass markers.

(JASCO, J-720). The far-UV CD spectra of the proteins were measured from 190 to 260 nm in 10 mM sodium phosphate buffer, pH 7.5. The instrument was set with 0.25 s response, 500 mdeg sensitivity, 50 nm/min speed, and 10 mm path length. An average of three scans was taken for each sample with 0.8–1 mg/ml protein concentration. The data were processed by subtracting the buffer spectrum.

RESULTS

Expression and purification of His_6–BjHMGS1

One of the four isolated *B. juncea* HMGS cDNAs [33], HMGS1 cDNA, was cloned in-frame in pET3a expression vector to yield plasmid pBj75. The 1.4 kb cDNA was fused to DNA encoding a His_6-tag at its 5′-end to enable easy purification of the recombinant protein using Ni^{2+}-NTA columns. Using the GCG computer analysis package, the predicted mass of this recombinant protein is 53 kDa, evident as a distinct band after SDS/PAGE (Figure 1, lanes 1 and 2) from bacterial soluble protein extracts of IPTG-induced BL21 Star (DE3) pLysS cells transformed with plasmid pBj75. On checking for HMGS activity *in vitro,* protein extracts from IPTG-induced cultures showed a significant increase in apparent activity (results not shown). In contrast, activity was absent in crude extracts from pET3a-transformed *E. coli*. Western-blot analysis using anti-peptide antibodies against BjHMGS1 detected a cross-reacting band (apparent molecular mass 53 kDa) in soluble protein extracts (Figure 1, lanes 3 and 4) and confirmed the identity of the protein. Batch extraction of recombinant His_6–BjHMGS1 was carried out 4 h after IPTG induction under non-denaturing conditions, and the protein was subsequently purified through an Ni^{2+}-NTA agarose column. The Coomassie Blue-stained gel showed purified His_6–BjHMGS1 with an apparent molecular mass of 53 kDa (Figure 1, lane 5). Purified His_6–BjHMGS1 (5 mg) was harvested from 1 litre of cell culture (Table 2), dialysed against 50 mM Tris buffer (pH 7.5) and used for *in vitro* assays.

Effect of cation concentration and F-244 on His_6–BjHMGS activity

In contrast with previously reported avian HMGS [16] and insect HMGS [38], which are activated by $MgCl_2$, His_6–BjHMGS1 did not require any cations for its activity. Of the cations (Mg^{2+}, Mn^{2+}, Co^{2+} and Zn^{2+}) tested, none exerted any stimulating effect on activity at 0.5–10 mM concentration, and all except Mg^{2+} were inhibitory. Mn^{2+} reduced activity to below 80 % at concentrations of 2 mM and above, while Zn^{2+} and Co^{2+} were significantly inhibitory even at a concentration of 0.5 mM.

In order to test the hypothesis that a firmly bound cation could be present at the enzyme and be essential for catalysis, we incubated the enzyme in the presence of a strong chelator, phenanthroline, which should have stripped off such a cofactor. We noted that treatment by phenanthroline led to some inactivation of enzyme activity, but a little stimulation by cations that were added after dialysis of the enzyme against a Tris buffer system was only observed with Mg^{2+}, while all others tested exhibited essentially the same effects as with untreated, purified His_6–BjHMGS1.

To test the effect of F-244 (= L-659,699), a β-lactone known to specifically inhibit HMGS [39,40], assays were carried out in the presence of varying concentrations (0–100 nM) of the compound. Measurement of His_6–BjHMGS1 activity in the presence of increasing concentrations of F-244 concentration revealed that it is a very effective inhibitor of His_6–BjHMGS1, with an IC_{50} value of 35 nM.

Table 2 Purification of His_6–BjHMGS1 from a 1 litre culture of pBj75-transformed *E. coli* BL21 Star (DE3) pLysS cells following induction with 0.5 mM IPTG

	Crude cell extract	Ni^{2+}-NTA purified fraction
Volume (ml)	24.5	5.5
Total protein (mg)	43.5	4.95
Total activity (μmol · min^{-1})	1.13	0.52
Specific activity (μmol · min^{-1} · mg^{-1})	0.02	0.10
Yield (%)	100.00	46.01

Enzyme activity was measured in the presence of equimolar concentrations of [^{14}C]acetyl-CoA and AcAc-CoA at 30 °C.

Effect of pH and temperature on His_6–BjHMGS1 activity

Recombinant His_6–BjHMGS1 showed a pH optimum of 8.5 (Figure 2A) and a temperature optimum of 35 °C (Figure 2B). We determined an apparent energy of activation of 62.5 J · mol^{-1} as calculated from the Arrhenius plot (Figure 2C). In preceding experiments we noted that freshly isolated His_6–BjHMGS1 was rapidly activated by about 8-fold upon preincubation for 5 min in the presence of 5 mM DTE, after which the activity remained constant.

Structural features of His_6–BjHMGS1

The molecular mass of the purified His_6–BjHMGS1 determined by non-denaturing PAGE was 106 kDa. Since its estimated subunit size on SDS/PAGE (Figure 1) was consistent with its calculated subunit size (53 kDa), it is predicted to be a homodimer.

Activity of recombinant His_6–BjHMGS1

HMGS activity was measured using the fixed-time radiochemical assay [15] in the presence of [^{14}C]acetyl-CoA and AcAc-CoA. Purified recombinant His_6–BjHMGS1 showed a specific activity of 0.106 μmol · min^{-1} · mg^{-1} with a 46 % recovery (Table 2). This purified protein was then used for kinetic assays. Kinetic analysis of His_6–BjHMGS1 revealed that AcAc-CoA exerts an inhibitory effect on its activity. Figure 3 shows double reciprocal plots of initial velocities versus varying concentrations of one substrate, while the other substrate was kept at constant. At the

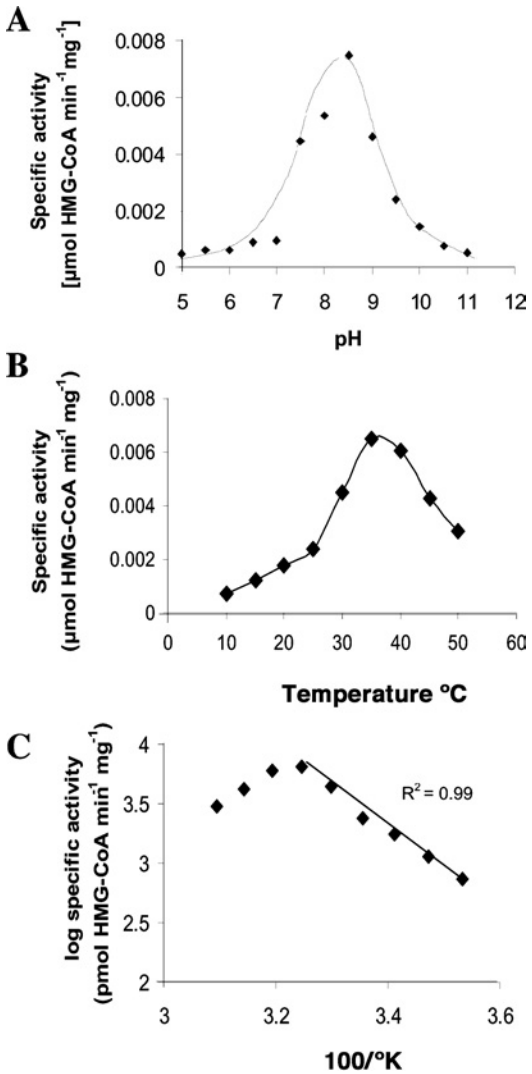

Figure 2 pH and temperature optimum of His_6–BjHMGS1

Assays were conducted in the presence of 75 ng of His_6–BjHMGS1 in 50 mM Tris/HCl (pH 7.5) and equimolar concentrations of [^{14}C]acetyl-CoA and AcAc-CoA at the indicated pH (**A**) and temperature (**B**) for 10 min. The slope as determined from the linear part of the corresponding Arrhenius plot (**C**) for the selected data from (**B**) yields a value of 62.51 J · mol^{-1} apparent activation energy in the presence of 5 mM DTE. In (**A**) and (**B**) the values represent an average of two to three independent assays.

concentrations tested (2.8–22.9 μM acetyl-CoA and 4.0–80.0 μM AcAc-CoA), we observed that the lower the concentration of the substrate acetyl-CoA in binding the enzyme, the more the second substrate AcAc-CoA became inhibitory (Figures 3A and 3B). Apparently, at low acetyl-CoA concentrations, AcAc-CoA can compete for the same binding site, yielding a dead-end complex, as was described for the yeast enzyme [23]. This resulted in increased sharp upward curving of lines in Lineweaver–Burk plots when AcAc-CoA concentration varied and acetyl-CoA was kept constant (Figure 3A). Likewise, by first increasing the concentration of substrate acetyl-CoA with that of AcAc-CoA kept constant, the enzyme was increasingly alleviated from substrate inhibition (Figure 3B), indicating that AcAc-CoA inhibition is competitive with respect to acetyl-CoA. A replot of slopes from Figure 3(B) versus varying AcAc-CoA concentrations yielded an apparent substrate inhibition constant $K_{\text{i-AcAc-CoA}}$ of 38 μM, an apparent $K_{\text{m-acetyl-CoA}}$ of 43 μM and a $V_{\max}$ of 0.47 μmol · min^{-1} · mg^{-1} (Table 3).

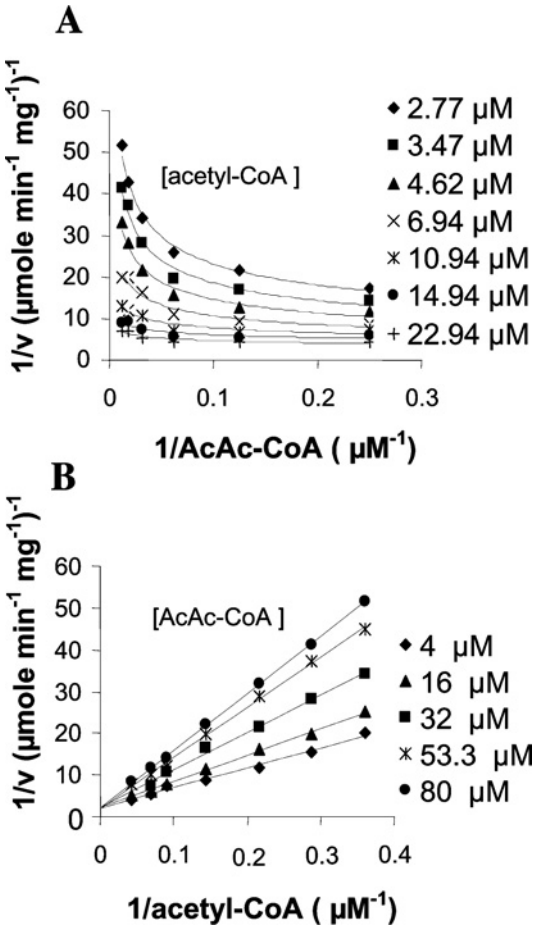

Figure 3 Determination of kinetic constants for His_6–BjHMGS1

Double-reciprocal plots showing the effect on His_6–BjHMGS1 activity at varying (**A**) AcAc-CoA concentrations and fixed acetyl-CoA concentration, or (**B**) acetyl-CoA concentrations and fixed AcAc-CoA concentration. Assays were carried out at the indicated concentrations of acetyl-CoA and AcAc-CoA, in the presence of 50 mM Tris/HCl (pH 7.5) and 75 ng of His_6–BjHMGS1 at 30 °C for 10 min.

Table 3 Kinetic properties of wild-type and mutant His_6–BjHMGS1

$V_{\max}$ and K_m were measured in the presence of variable concentrations of acetyl-CoA and AcAc-CoA employing a radiometric assay. Hydrolase activity (acetyl-CoA hydrolysis) was measured by converting the remaining [^{14}C]acetyl-CoA to acid stable citrate with excess citrate synthase and oxaloacetate [37]. n.i., no inhibition.

Enzyme	$V_{\max}$ (μmol · min^{-1} · mg^{-1})	$K_{\text{m-acetyl-CoA}}$ (μM)	$K_{\text{i-AcAc-CoA}}$ (μM)	K_{cat} (min^{-1}) ($V_{\max}$/[E])	acetyl-CoA hydrolysis ($t_{1/2}$)
Wild-Type	0.47	43	38	24.9	11.1
S89A	0.14	18	46	7.6	18.8
N115A	0.44	27	91	23.4	8.8
R157A	0.032	52	242	1.7	24.1
H188N	0.056	55	n.i.	2.9	61.7
C212S	0.078	29	39	4.1	14.7
S356A	0.30	26	199	16.1	25
S359A	4.04	24	28	214.1	4.7

His_6–BjHMGS1 is product-inhibited

To investigate whether His_6–BjHMGS1 exhibits product inhibition, different concentrations of HMG-CoA and HS-CoA (reduced CoA) were included in the reaction mixture and the

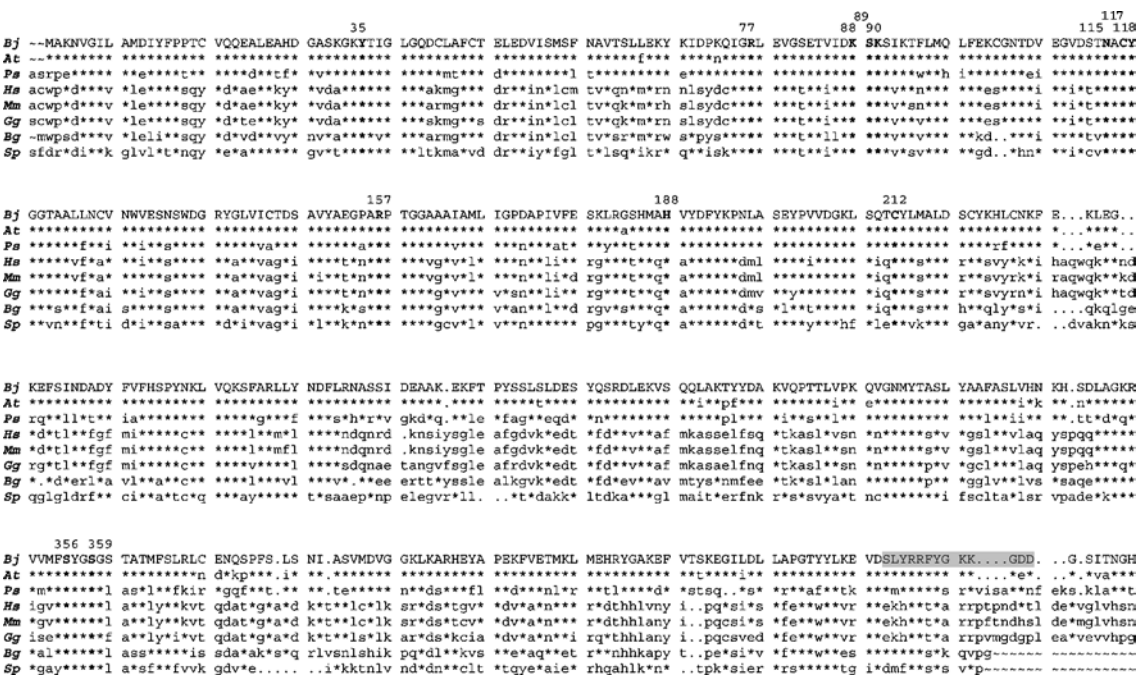

Figure 4 Alignment of deduced amino acid sequences for HMGS to indicate the locations of mutated amino acids

BjHMGS1 from *B. juncea* (*Bj*) [33]; HMGS from *A. thaliana* (*At*) [30]; *P. sylvestris* (*Ps*) [31]; *Homo sapiens* (*Hs*) [41]; *Mus musculus* (*Mm*) [42]; *Gallus gallus* (*Gg*) [43]; *B. germanica* (*Bg*) [44] and *Schizosaccharomyces pombe* (*Sp*) [45]. Amino acid residues selected for *in vitro* mutagenesis are in bold. The numbers on top correspond to the amino acid residues on BjHMGS1 and the shaded portion denotes peptide used for raising antibodies against BjHMGS1.

assay was carried out under standard conditions. The assays revealed that HMG-CoA and HS-CoA inhibit the enzyme in a concentration-dependent manner, with respect to acetyl-CoA. From plots of slopes over product concentrations, we calculated an apparent K_{is} of 9 μM for *R,S*-HMG-CoA and 80 μM for HS-CoA.

Expression, purification, and preliminary characterization of His_6–BjHMGS1 mutants

To investigate the significance of amino acid residues in His_6–BjHMGS1 that are conserved across species, *in vitro* mutagenesis was carried out. The amino acid residues chosen for site-directed mutagenesis were based on a comparison of BjHMGS1 with other known HMGS (Figure 4). BjHMGS1 shares a considerably significant homology with HMGS from *Arabidopsis thaliana* (94.6%), *P. sylvestris* (74.4%), human (48.5%), *Blatella germanica* (50.0%) and yeast (44.0%). The highest conservation with *A. thaliana* can be attributed to the fact that both plants belong to the family Brassicaceae. These conserved amino acid residues were targeted for mutagenesis because their side chains are likely to be involved in catalysis and recognition of ligands. Mutant forms of recombinant His_6–BjHMGS1, with single amino acid substitutions affecting each of the thirteen residues (Tyr-35, Arg-77, Lys-88, Ser-89, Lys-90, Asn-115, Cys-117, Tyr-118, Arg-157, His-188, Cys-212, Ser-356 and Ser-359) in BjHMGS1, were obtained and these amino acids are numbered according to native BjHMGS1 (Figure 4). Except for residues His-188 and Cys-212, all other substitutions were made with alanine, as it eliminates the side chain beyond the β-carbon without imposing severe constraints on secondary structure and tertiary conformation [46].

When expression constructs encoding each of thirteen mutant derivatives of His_6–BjHMGS1 were expressed in *E. coli*, only eight (S89A, K90A, N115A, R157A, H188N, C212S, S356A and S359A) of thirteen mutants could be expressed as soluble proteins. The remaining (Y35A, R77A, K88A, C117A and Y118A) accumulated only in the insoluble fractions and were not considered further. The Ni^{2+}-NTA-column-purified soluble mutant enzymes were essentially homogeneous by SDS/PAGE analysis (Figure 5A). Between 1 and 2 mg of purified enzyme was recovered from each 200 ml of culture. The apparent molecular masses of the mutant derivatives were estimated to be 53 kDa, in agreement with the calculated molecular mass (53 kDa) of His_6–BjHMGS1.

HMGS assays on the mutant enzymes were carried out using Ni^{2+}-NTA-column-purified enzymes and activities for all eight soluble mutant His_6–BjHMGS1 derivatives were measured under V_{max} conditions established for the wild-type. We observed that the activities of S89A, N115A and S356A were comparable with wild-type, whereas mutant K90A was completely inactive (Figure 5B). Mutants R157A, H188N and C212S exhibited more than 50% reduced activity compared with wild-type, while S359A increased activity significantly to 232% (Figure 5B).

Further kinetic analysis was carried out for each mutant at varying concentrations of both substrates, and the calculated kinetic constants are presented in Table 3. All amino acid substitutions, except R157A and H188N, displayed an approx. 2-fold decreased K_m-acetyl-CoA compared with wild-type (43 μM); R157A (52 μM) and H188N (55 μM) showed a slight increase (Table 3). Substitutions R157A, H188N and C212S exhibited 14-, 8- and 6-fold decreases in V_{max}, suggesting that these residues are directly or indirectly involved in the catalytic cycle. Replacement of S359 by an alanine residue caused a 10-fold increase in V_{max} with a $\sim$2-fold decrease in the affinity towards the substrate acetyl-CoA. Surprisingly, though H188N had a 6-fold decrease in V_{max} and an increased affinity for acetyl-CoA, it did not exhibit substrate inhibition by AcAc-CoA, in contrast with wild-type and the other mutant enzymes. Double reciprocal plots for H188N showed that its activity increased with an increase in AcAc-CoA concentration when acetyl-CoA concentration remained constant

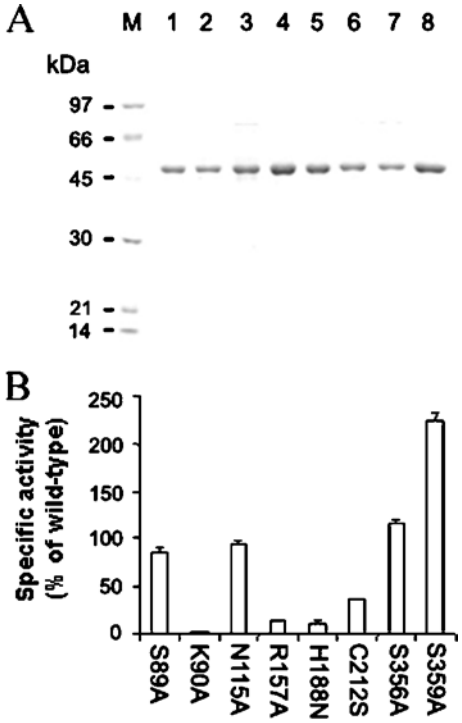

Figure 5 Expression and analysis of mutant derivatives of His_6–BjHMGS1

(**A**) Coomassie Blue-stanied SDS/PAGE of Ni^{2+}-NTA column-purified mutant proteins: S89A (lane 1), K90A (lane 2), N115A (lane 3), R157A (lane 4) H188N (lane 5), C212S (lane 6), S356A (lane 7) and S359A (lane 8). Lane M, protein standards including phosphorylase (97 kDa), BSA (66 kDa), ovalbumin (45 kDa) and carbonic anhydrase (30 kDa). Five micrograms of purified proteins were loaded per well. (**B**) Specific activities of mutant His_6–BjHMGS1 enzymes. Enzyme activities were measured in the presence of 250 ng of purified mutant proteins in 50 mM Tris/HCl (pH 7.5) and equimolar concentrations of [^{14}C]acetyl-CoA and AcAc-CoA at 30 °C for 10 min. The enzyme activity of mutants is expressed relative to the activity of wild-type His_6–BjHMGS1.

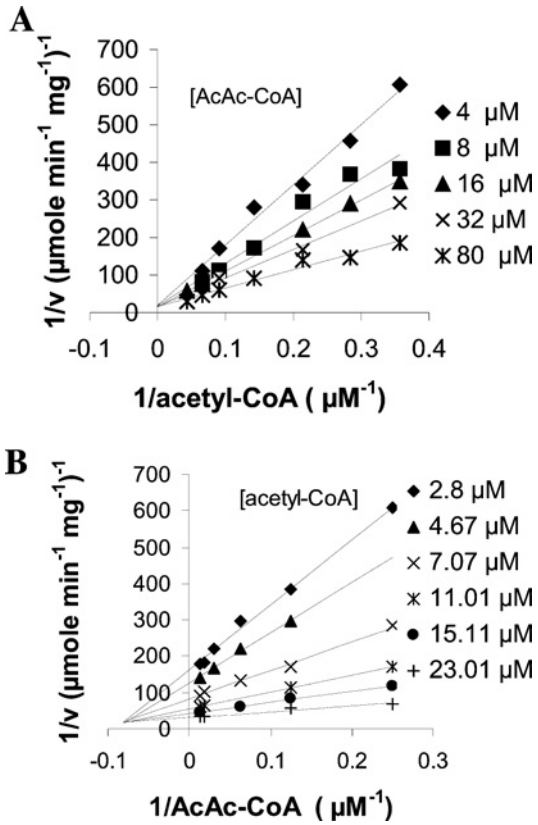

Figure 6 Determination of kinetic constants for H188N mutant

Double-reciprocal plots showing the effect on H188N activities at varying (**A**) AcAc-CoA concentrations at fixed acetyl-CoA concentration, or (**B**) acetyl-CoA concentrations at fixed AcAc-CoA concentration. Assays were carried out at the indicated concentrations of acetyl-CoA and AcAc-CoA in the presence of 50 mM Tris/HCl (pH 7.5) and 160 ng of H188N at 30 °C for 10 min.

(Figures 6A and 6B), apparently consistent with an ordered reaction mechanism, without the possible formation of a dead-end complex with AcAc-CoA before acetylation of the protein through reaction with acetyl-CoA. For this mutant enzyme we calculated an apparent K_m towards AcAc-CoA of about 12 μM (Table 4).

Construction, expression and kinetic analysis on the H188N/S359A mutant

The observations that amino acid substitutions H188N and S359A culminated in a lack of substrate inhibition for AcAc-CoA or an increased activity respectively, led us to design a double mutant having both these substitutions, to investigate if it rendered increased activity without AcAc-CoA inhibition. The S359A mutant plasmid was used as template for construction of a double mutant also having a H188N substitution. The resulting plasmid pBj110 carrying both substitutions, was expressed in *E. coli* and purified as described previously for His_6–BjHMGS1. Activity assays and kinetic analysis of H188N/S359A showed that it had increased activity with a 10-fold increase in V_{max}, characteristic of the S359A mutant, and a ~3-fold increase in $K_{m\text{-acetyl-CoA}}$ (Table 4). With respect to substrate inhibition by AcAc-CoA, H188N/S359A behaved similarly to the H188N mutant, now with a K_m of approx. 2.9 μM (Table 4); an increase in AcAc-CoA concentration at constant acetyl-CoA concentration resulted in increased activity of the enzyme, indicating that it has lost its AcAc-CoA inhibition property. Our results indicate that this double mutant has retained both properties conferred by substitutions H188N and S359A. This implies that substrate inhibition for AcAc-CoA is impaired by the H188N substitution.

Table 4 Comparison of kinetic properties of wild-type, H188N, S359A and H188N/S359A His_6–BjHMGS1

$K_{i\text{-HMG-CoA}}$ was determined in the presence of 16 μM AcAc-CoA and variable concentrations of acetyl-CoA and HMG-CoA. $K_{i\text{-HS-CoA}}$ was determined in the presence of 16 μM AcAc-CoA and variable concentrations of acetyl-CoA and HS-CoA. n.d., not determined; n.i., no inhibition.

	Wild-Type	H188N	S359A	H188N/S359A
$K_{i\text{-AcAc-CoA}}$ (μM)	38	n.i.	28	n.i.
$K_{i\text{-HMG-CoA}}$ (μM)	9	34	n.d.	38.9
$K_{i\text{-HS-CoA}}$ (μM)	80	n.d.	n.d.	n.d.
$K_{m\text{-acetyl-CoA}}$ (μM)	43	55	24	120
$K_{m\text{-AcAc-CoA}}$ (μM)	n.d.	12	n.d.	2.9
V_{max} (μmol · min^{-1} · mg^{-1})	0.47	0.056	4	4
K_{cat} (V_{max}/[E]) (min^{-1})	24	3	214	227
Acetyl-CoA hydrolysis ($t_{1/2}$)	11	61.76	4.7	6.7

Acetyl-CoA hydrolase activity

HMGS is known to catalyse a slow abortive hydrolysis of acetyl-CoA in formation of acetate and CoA, in the absence of a suitable acetyl group acceptor AcAc-CoA [24]. His_6–BjHMGS1 also

Table 5 Kinetic parameters of wild-type and mutant His_6–BjHMGS1

$\Delta(\Delta Gs)$, apparent difference in the free energy of the enzyme–substrate complex between wild-type and mutant enzyme, calculated from $\Delta(\Delta Gs) = RT \ln[(K_m)mut/(K_m)WT]$; $\Delta(\Delta G_T^{\#})$, apparent free-energy changes for the mutant enzyme relative to the wild-type enzyme for the transition state of the reaction calculated from $\Delta(\Delta G_T^{\#}) = -RT \ln[V/K]mut/(V/K)WT]$; $\Delta(\Delta G^{\#})$, apparent free energy changes for the mutant enzymes relative to the wild-type enzyme. $\Delta(\Delta G^{\#}) = \Delta G_T^{\#} - \Delta Gs = -RT \ln[V_{max},mut/V_{max},WT]$ (activation energy of the chemical step of bond making and breaking).

Enzyme	K_m (μM)	V_{max} (μmol · mg^{-1} · h)	(V_{max})mut/(V_{max})WT	$V_{max}/K_{m\ (ml/s*mg)}$	$\Delta(\Delta Gs)$ (kJ · mol^{-1})	$\Delta(\Delta G_T^{\#})$ (kJ · mol^{-1})	$\Delta(\Delta G^{\#})$ (kJ · mol^{-1})
WT	43	28.2	1.00	2357.72	0	0	0
S89A	18	8.5	0.30	1671.42	−2.13	+0.86	+2.99
N115A	27	26.4	0.93	3427.70	−1.11	−0.94	+0.17
R157A	52	1.9	0.06	131.40	0.51	+7.27	+6.76
H188N	55	3.3	0.11	219.43	0.62	+5.98	+5.36
C212S	29	4.6	0.16	578.37	−0.99	+3.54	+4.53
S356A	26	18.2	0.64	2482.57	−1.23	−0.13	+1.1
S359A	24	242.4	8.57	35 144.50	−1.39	−6.81	−5.33
H188N/S359A	120	257.4	9.11	7675.94	2.58	−2.96	−5.54

exhibits acetyl-CoA hydrolase activity which was measured by monitoring the disappearance of [^{14}C]acetyl-CoA, as determined by measuring residual [^{14}C]acetyl-CoA through its conversion into acid-stable form (citrate) in the presence of citrate synthase and oxaloacetate. The reaction proceeded to completion at 60 min with a $t_{1/2}$ of 11 min (Table 3). Enzymes H188N and S359A showed the lowest and highest acetyl-CoA hydrolase activity with a $t_{1/2}$ of 61.7 min (~6-fold decrease) and 4.7 min (~3-fold increase) respectively, consistent with their HMGS activity (Table 3). Mutants R157A and S356A displayed a ~2-fold decrease in acetyl-CoA hydrolase activity, whereas the remaining mutants (S89A, N115A and C212S) did not exhibit any significant change in their hydrolase activity (Table 3). The double mutant H188N/S359A had a similar level of hydrolase activity as that of S359A (Table 4).

Thermodynamic properties of His_6–BjHMGS1

It is evident from Table 5 that R157A, H188N and C212S substitutions destabilize the enzyme by 7.3 kJ · mol^{-1}, 6 kJ · mol^{-1} and 3.5 kJ · mol^{-1} respectively, thus leading to an increase in the activation energy of all the three substitutions (Table 5). In contrast, substitution of Ser-359 with an alanine residue stabilized the transition state of BjHMGS1 by 6.8 kJ · mol^{-1}, thus leading to a 5.3 kJ · mol^{-1} decrease in the activation energy (Table 5). The double mutation H188N/S359A caused a 2.6 kJ · mol^{-1} decrease in the apparent binding energy of substrate in the ground state and 3 kJ · mol^{-1} additional stabilization in the transition state, resulting in a decrease in the activation energy (Table 5).

CD spectroscopy on His_6–BjHMGS1 and its mutants

To investigate the effect of the amino acid substitutions on protein folding, CD spectra in the far-UV (190–260 nm) were measured. As illustrated in Figure 7, the far-UV spectra for recombinant His_6–BjHMGS1 and its variants were very similar, indicating that the amino acid substitutions had no impact on secondary structure. All the samples exhibited spectral minima near 210 and 223 nm.

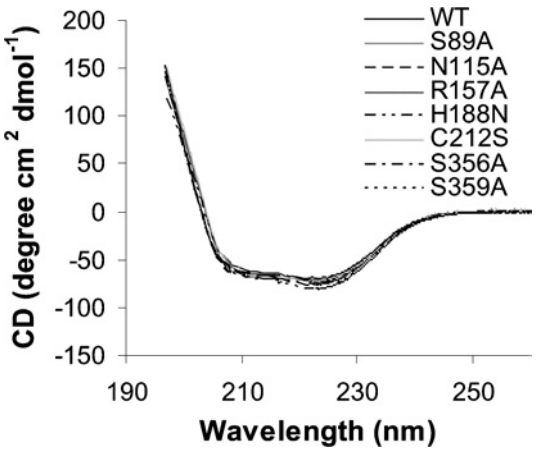

Figure 7 Far-UV CD spectroscopy of recombinant His_6–BjHMGS1 and its variants

Protein concentration used ranged from 0.8 to 1.0 mg/ml in 10 mM phosphate buffer and scanning was carried out at 22 °C using a 10 mm quartz cuvette. An average of three scans was taken for each sample, and the data were processed by subtracting the buffer spectrum.

DISCUSSION

In order to better understand the role of HMGS in plants, we sought to characterize BjHMGS1 by kinetic analysis and mutagenic studies. His_6–BjHMGS1 was expressed as a 53 kDa protein in IPTG-induced *E. coli* cultures. As the whole pathway from acetyl-CoA to MVA is absent in *E. coli* [6], the apparent activity we measured *in vitro* with crude extracts and purified protein was due to the expressed His_6–BjHMGS1. Cations did not have any stimulatory effect; instead they inhibited its activity, in contrast with cytosolic chicken liver HMGS [16] and *B. germanica* HMGS1 [38], which indicated 140% and 230% activation respectively in the presence of 20 mM $MgCl_2$. In its apparent independence from cations, the BjHMGS1 resembles the yeast enzyme [23] and the mitochondrial isoenzyme in animals [47]. The slight effect of reconstitution of apparent activity by Mg^{2+}, observed with the phenanthroline-treated BjHMGS1, was not really significant; furthermore, these observations allow us to argue for the absence of a firmly bound cation, while still remaining accessible to chelation by phenanthroline. At this point, however, we cannot yet exclude the presence of an intrinsic, cryptic cation, like in malate synthases, catalysing a Claisen-type condensation [48,49]. His_6–BjHMGS1 showed inhibition in the presence of F-244, a specific inhibitor of HMGS [39,40], as demonstrated with the human [50] and hamster [51] recombinant HMGS. Freshly isolated His_6–BjHMGS1 was activated by DTE, sharing the property of the sequel enzyme HMGR isolated from radish seedlings [52], i.e., to be active only in a reduced state. His_6–BjHMGS1 behaves as a homodimer (~106 kDa), consistent with observations made with HMGS purified from baker's yeast [22],

ox liver [53] and *Enterococcus faecalis* HMGS [54]; with DTE-activated enzyme we found an optimum activity at pH 8.5.

From what is known from yeast and animal HMGS proteins, the HMGS reaction should follow a simple Ping Pong Bi Bi mechanism, which perfectly well explains substrate inhibition by the second substrate [55], here AcAc-CoA [21,23], and irregular patterns in double-reciprocal plots. However, in the H188N mutant, substrate inhibition was lost, leading to intersecting patterns typical of ordered bi-substrate reactions, albeit at diminished catalytic efficiency. This pattern was maintained in the double mutant, but at increased catalytic capacity, although the apparent affinity towards acetyl-CoA was diminished by approx. 3-fold. If we follow the rule that a K_m like that of His_6–BjHMGS1 more or less reflects intracellular substrate concentrations, then this should be around 40 μM for acetyl-CoA, a value similar to that calculated for the yeast cytoplasm [23]. However, the equilibrium of the AACT reaction is by far on the side of acetyl-CoA formation [12,23]. In order to catalyse the reaction in the presence of presumably nanomolar concentrations [23], the affinity for AcAc-CoA must be extremely high, which seems true with wild-type BjHMGS1, but by the same token, this high affinity explains the substrate inhibition. Furthermore, that all substrates and products contain CoA, which might make it difficult for the protein to discriminate between the common structural features, must presumably lead to competition for the same binding sites, even if the CoA moiety might adopt bent or extended conformations. This explains the absence of consensus structure or sequence motifs in enzymes like malate synthase and others catalysing similar reactions [49].

Previous *in vitro* mutagenesis studies on avian HMGS have demonstrated that conserved amino acid residues (Glu-95, Cys-129 and His-264) are essential for catalytic activity [56–58]. These residues correspond to Glu-83, Cys-117 and His-247 in BjHMGS1 respectively. Cys-129 is an absolute requirement for the acetyl-*S*-enzyme reaction intermediate formation [56], while Glu-95 plays an important role in the chemistry of C–C bond formation [58]. Studies on conserved aromatic residues in avian HMGS, have revealed that Tyr-130 (corresponding to Tyr-118 in His_6–BjHMGS1) and Tyr-376 are part of the catalytic site [59]. In this study, kinetic analysis of thirteen invariant acidic residues revealed that the three mutants R157A, H188N and C212S displayed significant decreases in activity, indicating that they contribute to catalytic efficiency. From the fact that all these three amino acids lie near to each other, and that the disruption of any of them decreases catalytic efficiency, it can be inferred that they are essential for activity, without distinguishing their direct (catalytic and/or binding) or indirect (structural) role [60].

In avian HMGS, replacement of cysteine with alanine in Cys-59, Cys-224 and Cys-232 did not affect HMGS activity [61]. In contrast, a C212S substitution in His_6–BjHMGS1, which corresponds to Cys-224 of avian HMGS, significantly decreased its activity. As the amino acid structures of both cysteine and serine are similar except for the replacement of the SH-group in cysteine with an OH-group, it appears that Cys-212 has a role in catalysis in plant HMGS, or in the maintenance of a catalytically competent conformation. Substitution S359A increased the apparent V_{max} 10-fold with a corresponding increase in acetyl-CoA hydrolase activity as compared with wild-type His_6–BjHMGS1. In the absence of the second substrate AcAc-CoA, which acts as an acceptor for the acetyl group, His_6–BjHMGS1 catalyses a slow abortive hydrolysis of acetyl-CoA to form acetate and CoA, similarly to avian HMGS [37]. The reverse was observed with the H188N, which showed an $\sim$8-fold reduction in both HMGS and hydrolase activities, but this mutation rendered the enzyme insensitive to AcAc-CoA inhibition, unlike all other mutants that show AcAc-CoA inhibition being characteristic of the wild-type enzyme. Previous studies by substitution of histidine residues confirmed that His-264 in avian HMGS anchors the second substrate AcAc-CoA [57]. It also resulted in a higher K_m for acetyl-CoA, which may be due to diminished binding affinity of the second substrate to the free enzyme, i.e., accompanied by reduced substrate inhibition. In this study, the lack of AcAc-CoA inhibition in H188N suggests that this residue is involved in AcAc-CoA binding in native BjHMGS1. The double mutant H188N/S359A resulted in both higher activity (property of S359A) and lack of AcAc-CoA substrate inhibition (property of H188N), which on kinetic analysis revealed that it has a similar activity level to S359A, but lacks substrate inhibition by AcAc-CoA. Substitution resulting in lack of substrate inhibition has never been reported previously for any HMGS. From the viewpoint of evolution, there are probably some restrictions for the 'optimization' of the enzyme's catalytic efficiency, first through the quite limited availability of the second substrate AcAc-CoA in the cytoplasm, which requires strong affinity with K_m values that can be estimated as $\ll 1$ μM [23] (which on the other hand leads to substrate inhibition), but also avoiding hydrolysis of substrate(s), thereby wasting energy that had been invested into their synthesis.

It is evident that through exchange of these amino acids by site-directed mutagenesis some subtle mechanistic modifications can be induced. While it seems clear that acetyl-CoA has to bind first, the release of the HS-CoA before AcAc-CoA can bind might occur in parallel or even later, this at the expense of the enzyme's affinity for AcAc-CoA. In no case could we observe a clear parallel pattern in double-reciprocal plots, indicative of a Ping Pong mechanism. Although R157A, H188N, C212S and S359A substitutions affected His_6–BjHMGS1 activity, they had no effect on the secondary protein structure indicating that they did not affect the protein conformation. Within the limits of this method, the CD spectrum analyses of His_6–BjHMGS1 and its mutant derivatives revealed that there was no significant change in the secondary structure culminating from the amino acid substitutions, and the spectra are consistent with that of previously reported human HMGS which had spectral minima near 208 and 222 nm, characteristic of an α-helical structure [50]. The residues (Tyr-35, Arg-77, Lys-88, Cys-117 and Tyr-118), which, when exchanged with alanine, resulted in the formation of inclusion bodies, might well control the conformation of the enzyme. The exchange at those positions might lead to unfavourable folding and interactions between neighbouring protein molecules, which ultimately results in agglomeration. The elucidation of their precise role also awaits the structural characterization of plant HMGS.

From an Arrhenius plot we determined a free energy of activation of 62.5 $J \cdot mol^{-1}$ for His_6–BjHMGS1. Its temperature optimum profile is similar to that observed with HMGS from *E. faecalis* [54], who calculated a 25.1 $kJ \cdot mol^{-1}$ of energy of activation. The further thermodynamic data obtained with mutagenized enzyme forms support the hypothesis that Arg-157, His-188 and Cys-212 are important in His_6–BjHMGS1 catalytic activity. Keeping in mind the limits of such calculations [60], substitutions R157A, H188N and C212S appear to destabilize the enzyme, leading to an increase in the activation energy by all the three substitutions, suggesting that these residues are involved in stabilizing the transition state of His_6–BjHMGS1. In contrast, substitution S359A resulted in the stabilization of the transition state of His_6–BjHMGS1, leading to decreased activation energy. Furthermore, the double mutation H188N/S359A caused a decrease in the apparent binding energy of substrate in the ground state and additional stabilization in the transition state, resulting in

a decrease in activation energy. However, it has to be considered that so-called catalytic, binding, and structural residues are not acting independently [60].

Our results suggest that His-188 and Ser-359 residues in His_6–BjHMGS1 play a particularly important role in the regulation of HMGS activity in the cytoplasmic MVA pathway by conferring AcAc-CoA inhibition and lower activity respectively to HMGS. One further aspect needs to be well thought out: with the loss of substrate inhibition, the affinity for the products HMG-CoA and HS-CoA is also diminished. We are tempted to ascribe some regulatory function to the enzyme by itself, simply through its intrinsic kinetic properties. Such properties could have an important function in the regulation of the MVA pathway, for instance when the sequel enzyme HMGR is inhibited or down-regulated. Piling up substrates and products would immediately diminish HMGS activity *in vivo* and thereby avoid the risk of accumulation of potentially toxic intermediates. For rapid adaptation of varying flux rates from acetyl-CoA to HMG-CoA, this could happen without the need to proteolytically degrade the enzyme, and without involvement of processes such as phosphorylation and/or dephosphorylation or even *de novo* synthesis.

In conclusion, the biochemical characterization of His_6–BjHMGS1 reported here has shed some light on the nature of this enzyme in plants. Also, the use of *in vitro* mutagenesis in analysing the activity and kinetics of the various His_6–BjHMGS1 mutants has given us an insight into the structure–function relationship of this enzyme in plants. As this study reports the first characterized HMGS from plants, it should pave the way for a better understanding in the regulatory function of this enzyme in the plant MVA pathway.

This study is dedicated to Professor Harry Rudney (University of Cincinnati, CT, U.S.A.), in honour of his pioneering work in the enzymic synthesis of HMG-CoA and its conversion into MVA in yeast and vertebrate systems, and for having allowed one of us (T. J. B.) to introduce plant enzymology into his laboratory more than two decades ago. We thank Dr W. K. Yip for letting us use his liquid-scintillation counter, Dr H. Z. Sun for the provision of a spectropolarimeter and Dr W. T. Wong for a sample of phenanthroline (Department of Chemistry, The University of Hong Kong, China). We are indebted to Dr M. D. Greenspan and Dr S. B. Singh (Merck Sharp & Dohme Research Laboratories, Rahway, NJ, U.S.A.) for generous provision of F-244. This work was supported by the Research Grants Council of the Hong Kong Special Administrative Region, China (Project HKU7221/02M) and the France/Hong Kong Joint Research Scheme (F-HK A04/00). D. A. N. was supported by a studentship from the University of Hong Kong.

REFERENCES

1 Bach, T. J. (1995) Some new aspects of isoprenoid biosynthesis in plants: a review. Lipids **30**, 191–202
2 Kessler, A. and Baldwin, I. T. (2002) Plant responses to insect herbivory: the emerging molecular analysis. Annu. Rev. Plant Biol. **53**, 299–328
3 Bochar, D. A., Freisen, J. A., Stauffacher, C. V. and Rodwell, V. W. (1999) Biosynthesis of mevalonic acid from acetyl-CoA. In Comprehensive Natural Products Chemistry (Barton, D. and Nakanishi, K., eds.), vol 2, pp. 15–44, Elsevier Science Ltd
4 Rohmer, M., Knani, M., Simonin, P., Sutter, B. and Sahm, H. (1993) Isoprenoid biosynthesis in bacteria: a novel pathway for the early steps leading to isopentenyl diphosphate. Biochem. J. **295**, 517–524
5 Lichtenthaler, H. K. (1999) The 1-deoxy-D-xylulose-5-phosphate pathway of isoprenoid biosynthesis in plants. Annu. Rev. Plant Physiol. Plant Mol. Biol. **50**, 47–65
6 Rohmer, M. (1999) The discovery of a mevalonate-independent pathway for isoprenoid biosynthesis in bacteria, algae and higher plants. Nat. Prod. Rep. **16**, 565–574
7 Kuzuyama, T. and Seto, H. (2003) Diversity of the biosynthesis of the isoprene units. Nat. Prod. Rep. **20**, 171–183
8 Hemmerlin, A. and Bach, T. J. (1998) Effects of mevinolin on cell cycle progression and viability of tobacco BY-2 cells. Plant J. **14**, 65–74
9 Hemmerlin, A., Brown, S. C. and Bach, T. J. (1999) Function of mevalonate in tobacco cell proliferation. Acta. Bot. Gall. **146**, 85–100
10 Hemmerlin, A., Hoeffler, J. F., Meyer, O., Tritsch, D., Kagan, I. A., Grosdemange-Billiard, C., Rohmer, M. and Bach, T. J. (2003) Cross-talk between the cytosolic mevalonate and the plastidial methylerythritol phosphate pathways in tobacco bright yellow-2 cells. J. Biol. Chem. **250**, 5768–5773
11 Laule, O., Fürholz, A., Chang, H.-S., Zhu, T., Wang, X., Heifetz, P. B., Gruissem, W. and Lange, B. M. (2003) Cross-talk between cytosolic and plastidial pathways of isoprenoid biosynthesis in *Arabidopsis thaliana*. Proc. Natl. Acad. Sci. U.S.A. **100**, 6866–6871
12 Lynen, F., Henning, U., Bublitz, C., Sorbö, B. and Kröplin-Rueff, L. (1958) Der chemische mechanismus der acetessigsäurebildung in der leber. Biochem. Z. **330**, 269–294
13 Clinkenbeard, K. D., Sugiyama, T., Moss, J., Reed, W. D. and Lane, M. D. (1973) Molecular and catalytic properties of cytosolic acetoacetyl coenzyme A thiolase from avian liver. J. Biol. Chem. **248**, 2275–2284
14 Rudney, H. (1957) The biosynthesis of β-hydroxy-β-methylglutaric acid. J. Biol. Chem. **227**, 363–377
15 Clinkenbeard, K. D., Reed, W. D., Mooney, R. A. and Lane, M. D. (1975) Intracellular localization of the 3-hydroxy-3-methylglutaryl coenzyme A cycle enzymes in liver. Separate cytoplasmic and mitochondrial 3-hydroxy-3-methylglutaryl coenzyme A generating systems for cholesterogenesis and ketogenesis. J. Biol. Chem. **250**, 3108–3116
16 Clinkenbeard, K. D., Sugiyama, T., Mooney, R. A. and Lane, M. D. (1975) Cytoplasmic 3-hydroxy-3-methylglutaryl coenzyme A synthase from liver. Purification, properties, and role in cholesterol synthesis. J. Biol. Chem. **250**, 3124–3135
17 Bach, T. J., Boronat, A., Caelles, C., Ferrer, A., Weber, T. and Wettstein, A. (1991) Aspects related to mevalonate biosynthesis in plants. Lipids **26**, 637–648
18 Ferguson, Jr, J. J. and Rudney, H. (1959) The biosynthesis of β-hydroxy-β-methylglutaryl coenzyme A I. Identification and purification of the hydroxymethylglutaryl coenzyme A condensing enzyme. J. Biol. Chem. **234**, 1072–1075
19 Rudney, H. and Ferguson, J. J. (1959) The biosynthesis of β-hydroxy-β-methylglutaryl coenzyme A in yeast II. The formation of hydroxymethylglutaryl coenzyme A via condensation of acetyl coenzyme A and acetoacetyl coenzyme A. J. Biol. Chem. **234**, 1076–1080
20 Stewart, P. R. and Rudney, H. (1966a) The biosynthesis of β-hydroxy-β-methylglutaryl coenzyme A in yeast III. Purification and properties of the condensing enzyme thiolase system. J. Biol. Chem. **241**, 1212–1221
21 Stewart, P. R. and Rudney, H. (1966b) The biosynthesis of β-hydroxy-β-methylglutaryl coenzyme A in yeast IV. The origin of the thioester bond of β-hydroxy-β-methylglutaryl coenzyme A. J. Biol. Chem. **241**, 1222–1225
22 Middleton, B. and Tubbs, P. K. (1972) The purification and some properties of 3-hydroxy-3-methylglutaryl-coenzyme A synthase from baker's yeast. Biochem. J. **126**, 27–34
23 Middleton, B. (1972) The kinetic mechanism of 3-hydroxy-3-methylglutaryl-coenzyme A synthase from baker's yeast. Biochem. J. **126**, 35–47
24 Middleton, B. (1974) The kinetic mechanism and properties of the cytoplasmic acetoacetyl-coenzyme A thiolase from rat liver. Biochem. J. **139**, 109–121
25 Miziorko, H. M. and Lane, M. D. (1977) 3-Hydroxy-3-methylglutaryl-CoA synthase. Participation of acetyl-*S*-enzyme and enzyme-*S*-hydroxymethylglutaryl-SCoA intermediates in the reaction. J. Biol. Chem. **252**, 1414–1420
26 Lynen, F. (1967) Biosynthetic pathways from acetate to natural products. Activity of enzymes in rubber biosynthesis. Pure Appl. Chem. **14**, 137–167
27 Van der Heijden, R., Verpoorte, R. and Duine, J. A. (1994) Biosynthesis of 3-hydroxy-3-methylglutaryl-coenzyme A in *Catharanthus roseus*: acetoacetyl-CoA thiolase and HMG-CoA synthase show similar chromatographic behaviour. Plant Physiol. Biochem. **32**, 807–812
28 Suvachittanont, W. and Wititsuwannakul, R. (1995) 3-Hydroxy-3-methylglutaryl-coenzyme A synthase in *Hevea brasiliensis*. Phytochemistry **40**, 757–761
29 Weber, T. and Bach, T. J. (1994) Conversion of acetyl-coenzyme A into 3-hydroxy-3-methylglutaryl-coenzyme A in radish seedlings. Evidence of a single monomeric protein catalyzing a FeII/quinone-stimulated double condensation reaction. Biochim. Biophys. Acta. **1211**, 85–96
30 Montamat, F., Guilloton, M., Karst, F. and Delrot, S. (1995) Isolation and characterization of a cDNA encoding *Arabidopsis thaliana* 3-hydroxy-3-methylglutaryl-coenzyme A synthase. Gene **167**, 197–201
31 Wegener, A., Gimbel, W., Werner, T., Hani, J., Ernst, D. and Sandermann, Jr, H. (1997) Molecular cloning of ozone-inducible protein from *Pinus sylvestris* L. with high sequence similarity to vertebrate 3-hydroxy-3-methylglutaryl-CoA-synthase. Biochim. Biophys. Acta. **1350**, 247–252
32 Suwanmanee, P., Suvachittanont, W. and Fincher, G. B. (2002) Molecular cloning and sequencing of a cDNA encoding 3-hydroxy-3-methylglutaryl coenzyme A synthase from *Hevea brasiliensis* (HBK). Mull Arg. Science Asia **28**, 29–36
33 Alex, D., Bach, T. J. and Chye, M. L. (2000) Expression of *Brassica juncea* 3-hydroxy-3-methylglutaryl CoA synthase is developmentally regulated and stress-responsive. Plant J. **22**, 415–426

34 Bradford, M. M. (1976) A rapid and sensitive method for the quantitation of microgram quantities of protein utilizing the principle of protein-dye binding. Anal. Biochem. **72**, 248–254
35 Sambrook, J., Fritsch, E. F. and Maniatis, T. (1989), Molecular Cloning: A Laboratory Manual. Cold Spring Harbor Laboratory Press, Cold Spring Harbor, NY
36 Gallangher, S. R. (1995) Current protocols in protein science. Native discontinuous electrophoresis and generation of molecular-mass standard curves (Ferguson plots), p. 10.3.5, John Wiley & Sons, NY
37 Miziorko, H. M., Clinkenbeard, K. D., Reed, W. D. and Lane, M. D. (1975) 3-Hydroxy-3-methylglutaryl coenzyme A synthase. Evidence for an acetyl-*S*-enzyme intermediate and identification of a cysteinyl sulfhydryl as the site of acetylation. J. Biol. Chem. **250**, 5768–5773
38 Cabano, J., Buesa, C., Hegardt, F. G. and Marrero, P. F. (1997) Catalytic properties of recombinant 3-hydroxy-3-methylglutaryl coenzyme A synthase-1 from *Blattella germanica*. Insect. Biochem. Mol. Biol. **27**, 499–505
39 Greenspan, M. D., Yudkovitz, J. B., Lo, C. Y., Chen, J. S., Alberts, A. W., Hunt, V. M., Chang, M. N., Yang, S. S., Thompson, K. L. and Chiang, Y. C. (1987) Inhibition of hydroxymethylglutaryl-coenzyme A synthase by L-659,699. Proc. Natl. Acad. Sci. U.S.A. **84**, 7488–7492
40 Tomoda, H., Kumagai, H., Tanaka, H. and Omura, S. (1987) F-244 specifically inhibits 3-hydroxy-3-methylglutaryl coenzyme A synthase. Biochim Biophys Acta. **922**, 351–356
41 Russ, A. P., Ruzicka, V., Maerz, W., Appelhans, H. and Gross, W. (1992) Amplification and direct sequencing of a cDNA encoding human cytosolic 3-hydroxy-3-methylglutaryl-coenzyme A synthase. Biochim. Biophys. Acta. **1132**, 329–331
42 Boukaftane, Y., Duncan, A., Wang, S., Labuda, D., Robert, M. F., Sarrazin, J., Schappert, K. and Mitchell, G. A. (1994) Human mitochondrial HMG-CoA synthase: liver cDNA and partial genomic cloning, chromosome mapping to 1p12–p13, and possible role in vertebrate evolution. Genomics **23**, 552–559
43 Kattar-Cooley, P. A., Wang, H. H., Mende-Mueller, L. M. and Miziorko, H. M. (1990) Avian liver 3-hydroxy-3-methylglutaryl-CoA synthase: distinct genes encode the cholesterogenic and ketogenic isozymes. Arch. Biochem. Biophys. **283**, 523–529
44 Martinez-Gonzalez, J., Buesa, C., Piulachs, M. D., Belles, X. and Hegardt, F. G. (1993) 3-Hydroxy-3-methylglutaryl-coenzyme-A synthase from *Blattella germanica.* Cloning, expression, developmental pattern and tissue expression. Eur. J. Biochem. **217**, 691–699
45 Katayama, S., Adachi, N., Takao, K., Nakagawa, T., Matsuda, H. and Kawamukai, M. (1995) Molecular cloning and sequencing of the *hcs* gene, which encodes 3-hydroxy-3-methylglutaryl coenzyme A synthase of *Schizosaccharomyces pombe*. Yeast **11**, 1533–1537
46 Park, Y. S., Gee, P., Sanker, S., Schurter, E. J., Zuiderweg, E. R. and Kent, C. (1997) Identification of functional conserved residues of CTP: glycerol-3-phosphate cytidylyltransferase. Role of histidines in the conserved HXGH in catalysis. J. Biol. Chem. **272**, 15161–15166
47 Hegardt, F. G. (1999) Review: Mitochondrial 3-hydroxy-3-methylglutaryl-CoA synthase: a control enzyme in ketogenesis. Biochem. J. **338**, 569–582
48 Howard, B. R., Endrizzi, J. A. and Remington, S. J. (2000) Crystal structure of *Escherichia coli* malate synthase G complexed with magnesium and glyoxylate at 2.0 A resolution: Mechanistic implications. Biochemistry **39**, 3156–3168
49 Smith, C. V., Huang, C., Miczak, A., Russell, D. G., Sacchetini, J. C. and Höner zu Bentrup, K. (2003) Biochemical and structural studies of malate synthase from *Mycobacterium tuberculosis*. J. Biol. Chem. **278**, 1735–1743
50 Rokosz, L. L., Boulton, D. A., Butkiewicz, E. A., Sanyal, G., Cueto, M. A., Lachance, P. A. and Hermes, J. D. (1994) Human cytoplasmic 3-hydroxy-3-methylglutaryl coenzyme A synthase: expression, purification, and characterization of recombinant wild-type and Cys129 mutant enzymes. Arch. Biochem. Biophys. **312**, 1–13
51 Tomoda, H., Ohbayashi, N., Morikawa, Y., Kumagai, H. and Omura, S. (2004) Binding site for fungal beta-lactone hymeglusin on cytosolic 3-hydroxy-3-methylglutaryl coenzyme A synthase. Biochim Biophys Acta. **1636**, 22–28
52 Bach, T. J., Rogers, D. H. and Rudney, H. (1986) Detergent-solubilization, purification, and characterization of membrane-bound 3-hydroxy-3-methylglutaryl coenzyme A reductase from radish seedlings. Eur. J. Biochem. **154**, 103–111
53 Lowe, D. M. and Tubbs, P. K. (1985) 3-Hydroxy-3-methylglutaryl-coenzyme A synthase from ox liver. Purification, molecular and catalytic properties. Biochem. J. **227**, 591–599
54 Sutherlin, A., Hedl, M., Sanchez-Neri, B., Burgner, J. W., Stauffacher, C. V. and Rodwell, V. W. (2002) *Enterococcus faecalis* 3-hydroxy-3-methylglutaryl coenzyme A synthase, an enzyme of isopentenyl diphosphate biosynthesis. J. Bacteriol. **184**, 4065–4070
55 Segel, I. H. (1975) Enzyme kinetics. Behavior and analysis of rapid equilibrium and steady-state enzyme systems. John Wiley & Sons, New York
56 Misra, I., Narasimhan, C. and Miziorko, H. M. (1993) Avian 3-hydroxy-3-methylglutaryl-CoA synthase. Characterization of a recombinant cholesterogenic isozyme and demonstration of the requirement for a sulfhydryl functionality in formation of the acetyl-enzyme reaction intermediate. J. Biol. Chem. **268**, 12129–12135
57 Misra, I. and Miziorko, H. M. (1996) Evidence for the interaction of avian 3-hydroxy-3-methylglutaryl-CoA synthase histidine 264 with acetoacetyl-CoA. Biochemistry **35**, 9610–9616
58 Chun, K. Y., Vinarov, D. A. and Miziorko, H. M. (2000) 3-Hydroxy-3-methylglutaryl-CoA synthase: participation of invariant acidic residues in formation of the acetyl-*S*-enzyme reaction intermediate. Biochemistry **39**, 14670–14681
59 Misra, I., Wang, C. Z. and Miziorko, H. M. (2003) The influence of conserved aromatic residues in 3-hydroxy-3-methylglutaryl-CoA synthase. J. Biol. Chem. **278**, 26443–26449
60 Kraut, D. A., Caroll, K. S. and Herschlag, D. (2003) Challenges in enzyme mechanism and energetics. Annu. Rev. Biochem. **72**, 517–571
61 Misra, I., Charlier, Jr, H. A. and Miziorko, H. M. (1995) Avian cytosolic 3-hydroxy-3-methylglutaryl-CoA synthase: evaluation of the role of cysteines in reaction chemistry. Biochimica et Biophysica Acta **1247**, 253–259

Received 30 April 2004/25 June 2004; accepted 2 July 2004
Published as BJ Immediate Publication 2 July 2004, DOI 10.1042/BJ20040721